Glycobiology, 2018, vol. 28, no. 6, 406–417
doi: 10.1093/glycob/cwy025
Advance Access Publication Date: 6 April 2018
Original Article

Immunology

Airway glycomic and allergic inflammatory consequences resulting from keratan sulfate galactose 6-*O*-sulfotransferase (*CHST1*) deficiency

Tadahiro Kumagai[2,†], Takumi Kiwamoto[3,6,†], Mary E Brummet[3], Fan Wu[3], Kazuhiro Aoki[2], Zhou Zhu[3,7], Bruce S. Bochner[3,4,‡], and Michael Tiemeyer[2,5,1,‡]

[2]Complex Carbohydrate Research Center, University of Georgia, 315 Riverbend Road, Athens, GA 30602, [3]Department of Medicine, Division of Allergy and Clinical Immunology, The Johns Hopkins University School of Medicine, 5501 Hopkins Bayview Circle, Baltimore, MD 21224, [4]Department of Medicine, Division of Allergy-Immunology, Northwestern University Feinberg School of Medicine, 240 E. Huron Street, Room M-306, Chicago, IL 60611, and [5]Department of Biochemistry and Molecular Biology, University of Georgia, B122 Life Sciences Building, Athens, GA 30602, USA

[1]To whom correspondence should be addressed: Tel: 706-542-2740, Fax: 706-542-4401; e-mail: mtiemeyer@ccrc.uga.edu

[6]Current address: Department of Pulmonary Medicine, Faculty of Medicine, University of Tsukuba, 1-1-1 Tennodai, Tsukuba, Ibaraki 305-8575, Japan

[7]Current address: Departments of Internal Medicine and Pediatrics, Section of Allergy and Clinical Immunology, Yale University School of Medicine, 300 Cedar Street, TAC S469B, New Haven, CT 06511, USA

[†]These authors contributed equally to the manuscript as first authors.

[‡]These authors contributed equally to the manuscript as senior authors.

Received 16 May 2017; Revised 9 March 2018; Editorial decision 10 March 2018; Accepted 26 March 2018

Abstract

Siglec-F is a pro-apoptotic receptor on mouse eosinophils that recognizes 6′-sulfated sialyl Lewis X and 6′-sulfated sialyl *N*-acetyl-lactosamine as well as multivalent sialyl *N*-acetyl-lactosamine structures on glycan arrays. We hypothesized that attenuation of the carbohydrate sulfotransferase 1 (*CHST1*) gene encoding keratan sulfate galactose 6-*O*-sulfotransferase, an enzyme likely required for 6′-sulfation of some of these putative Siglec-F glycan ligands, would result in decreased Siglec-F lung ligand levels and enhanced allergic eosinophilic airway inflammation. Tissue analysis detected *CHST1* expression predominantly not only in parenchymal cells but not in airway epithelium, the latter being a location where Siglec-F ligands are located. Western blotting of lung extracts with Siglec-F–Fc fusion proteins detected ≈500 kDa and ≈200 kDa candidate Siglec-F ligands that were not appreciably altered in *CHST1*$^{-/-}$ lungs compared with normal mouse lungs. Characterization of the O-linked glycans of lung tissue and bronchoalveolar lavage fluid detected altered sialylation but minimal change in sulfation. Eosinophilic airway inflammation was induced in wild-type (WT) and *CHST1*$^{-/-}$ mice via sensitization to ovalbumin (OVA) and repeated airway challenge. After OVA sensitization and challenge, Siglec-F ligands on airway cells, and numbers of eosinophils and neutrophils accumulating in the airways, both increased to a similar degree in WT and *CHST1*$^{-/-}$ mouse lungs, while macrophages and lymphocytes increased significantly more in *CHST1*$^{-/-}$ mouse airway compared with normal mouse lungs. Therefore,

keratan sulfate galactose 6-*O*-sulfotransferase does not contribute to the synthesis of glycan ligands for Siglec-F in the airways, although its absence results in exaggerated accumulation of airway macrophages and lymphocytes.

Key words: asthma, *CHST1*, eosinophils, *O*-glycan, Siglec-F

Introduction

Both mouse Siglec-F and its closest functional paralog, human Siglec-8, are single-pass transmembrane cell surface proteins primarily expressed on the surface of eosinophils (Bochner 2009). Based on glycan array screening, Siglec-F and Siglec-8 recognize the same sialylated glycan ligands, namely 6′-sulfated sialyl Lewis X and 6′-sulfated sialyl *N*-acetyllactosamine (6′-su-sLe^x and 6′-su-LacNAc, respectively); Siglec-F, unlike Siglec-8, is also able to recognize nonsulfated, sialylated, multiantennary, complex N-linked glycans (Bochner et al. 2005; Tateno et al. 2005; Kiwamoto et al. 2014). Because engagement of Siglec-F or Siglec-8 induces eosinophil apoptosis (Nutku et al. 2003, 2005; Zhang et al. 2007; Nutku-Bilir et al. 2008; Zimmermann et al. 2008; Na et al. 2012), understanding their endogenous natural ligands and what controls their synthesis may shed light on how eosinophilic inflammation is regulated and controlled within tissues (Kiwamoto et al. 2013). Taking into account the candidate ligands identified so far, including specific sialylated mucins (Kiwamoto et al. 2015), their structures suggest that specific sulfotransferases and sialyltransferases will be necessary to generate ligands for Siglec-F and Siglec-8 in vivo (Patnode, Cheng et al. 2013; Kiwamoto et al. 2013, 2015). To date, studies have identified constitutive and Th2 cytokine-inducible lung epithelial ligands for Siglec-F that contain α2,3-linked terminal sialic acid residues and require the α2,3 sialyltransferase ST3Gal-III for their synthesis (Zhang et al. 2007; Cho et al. 2010; Guo et al. 2011; Suzukawa et al. 2013; Kiwamoto et al. 2014). Given the high-avidity binding of Siglec-F and Siglec-8 to arrayed glycans carrying 6′-sulfate (6′-su-sLe^x and 6′-su-LacNAc; Bochner et al. 2005; Tateno et al. 2005; Kiwamoto et al. 2014), a likely candidate for production of endogenous ligands is keratan sulfate galactose 6-*O*-sulfotransferase, encoded by the carbohydrate sulfotransferase 1 gene *CHST1* (Patnode, Cheng et al. 2013). We therefore, hypothesized that deletion of the *CHST1* gene would decrease Siglec-F airway ligand levels and selectively enhance eosinophilic airway inflammation. However, our results demonstrate that this enzyme is dispensable for generating Siglec-F ligands in mouse lung, a result previously reported in the same mouse model (Patnode, Cheng et al. 2013). In addition, we now demonstrate that the absence of the enzyme has no impact on allergic eosinophilic lung inflammation, further supporting earlier observations that endogenous lung ligands for Siglec-F may not contain 6′-sulfated sialoside structures, such as 6′-su-sLe^x and 6′-su-LacNAc, as previously assumed (Patnode, Cheng et al. 2013; Kiwamoto et al. 2015). Finally, we demonstrate that loss of *CHST1* was accompanied by collateral changes in glycoprotein *O*-glycosylation and in the cellularity of the airways in inflammation.

Results

The CHST1 gene is strongly expressed in lung parenchyma but not in airway epithelium

We obtained heterozygous mice carrying a *CHST1* knockout allele from the NIH Knockout Mouse Project at the University of California, Davis. In the targeted allele of these mice, the entire *CHST1* coding sequence has been replaced by an *Escherichia coli* beta-galactosidase reporter and a neomycin selection cassette (Patnode, Yu et al. 2013). Therefore, we mapped the distribution of *CHST1* gene expression by X-Gal staining in lung and trachea of genotyped animals. Strong staining of lung parenchyma was seen in *CHST1*$^{-/-}$ mice samples, but not in WT lung (Figure 1A and B), consistent with previous reports (Patnode, Cheng et al. 2013). There was no detectable staining of airway epithelium in *CHST1*$^{-/-}$ mice (Figure 1B), in contrast to previous studies using a polyclonal anti-*CHST1* antibody and immunohistochemistry that resulted in airway epithelial staining (Guo et al. 2011). Staining was also observed in both WT and *CHST1*$^{-/-}$ mouse trachea and tracheal submucosal glands (Figure 1A and C) suggesting, at least in these tissues, that staining with X-gal was nonspecific.

Loss of *CHST1* induces changes in the *O*-glycome of lung and bronchoalveolar lavage fluid

To assess the diversity of O-linked glycan structures expressed in the airway of WT and *CHST1*$^{-/-}$ mice, total glycoproteins were harvested from lung tissue (including epithelium and parenchyma) and from bronchoalveolar lavage (BAL) fluid. *O*-glycans were subsequently released from the harvested glycoproteins by reductive β-elimination, derivatized by permethylation and analyzed by nanospray ionization-multidimensional mass spectrometry (NSI-MS^n). Quantification of the full MS profiles of *O*-glycans released from WT and *CHST1*$^{-/-}$ mouse lung tissues revealed grossly similar profiles, although a modest trend toward increased sialylation of core 1 disaccharide was detected. The *CHST1*$^{-/-}$ mouse lung expressed decreased levels of monosialyl- and increased levels of disialyl core 1 disaccharide compared with WT, while the abundances of asialo-core 1 disaccharide and asialo-core 2 trisaccharide were slightly decreased in the *CHST1*$^{-/-}$ lung (Figure 2).

Previous characterization of endogenous airway ligands for Siglec-F identified a secreted mucin, Muc5B, as a major counter-receptor that carried glycans recognized by Siglec-F (Kiwamoto et al. 2015). Therefore, we assessed the glycan diversity in BAL fluid harvested from WT and *CHST1*$^{-/-}$ mice to further determine whether *CHST1* might be responsible for generating glycan ligands for Siglec-F. *O*-glycans released from BAL fluid glycoproteins were separated into nonsulfated and sulfated species by phase partition following permethylation and analyzed separately by NSI-MS^n. Full MS profiles revealed changes in nonsulfated *O*-glycan sialylation (Figure 3). While neutral core 1 and core 2 structures, as well as monosialylated core 2 structures, were unchanged in abundance between WT and *CHST1*$^{-/-}$ BAL fluid, a substantial decrease in mono- and disialyl core 1 disaccharide was detected in *CHST1*$^{-/-}$ BAL fluid compared with WT (Figure 4).

The most abundant sulfated, sialylated *O*-glycans in WT and *CHST1*$^{-/-}$ BAL fluid were identified as a minimally extended core 2 glycan ($Su_1NeuAc_1Hex_2HexNAc_2$, detected at m/z = 1386) and as the same core structure extended by an additional LacNAc

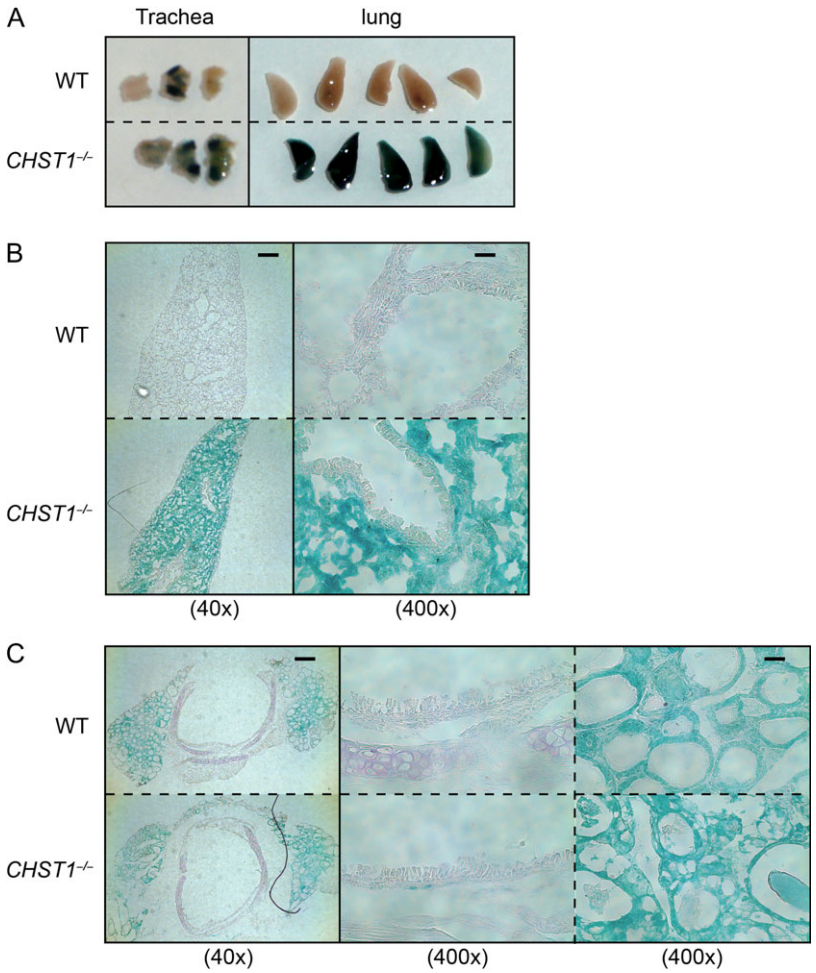

Fig. 1. Localization of keratan sulfate galactose 6-*O*-sulfotransferase (*CHST1*) expression in mouse lung and trachea. Tissues from WT and *CHST1*$^{-/-}$ mice were analyzed for β-galactosidase activity using X-Gal (blue staining) and revealed diffuse expression in lung parenchyma (Panel **A**) but not in epithelial cells (Panel **B**). Similar analysis of trachea and tracheal submucosal glands revealed diffuse staining of glands in both WT and *CHST1*$^{-/-}$ mice (Panel **C**) suggesting the presence of endogenous β-galactosidase activity in both strains of mice. Scale bars correspond to 100 μm for images at 40× magnification and 10 μm for images at 400× magnification in panels B and C.

($Su_1NeuAc_1Hex_3HexNAc_3$, detected at *m/z* = 1835). The abundance of the sulfated, minimally extended glycan (*m/z* = 1386) was only mildly affected in the *CHST1*$^{-/-}$ BAL fluid (Figure 5). However, the LacNAc-extended form of this sulfated glycan (*m/z* = 1835) was substantially reduced in the *CHST1*$^{-/-}$ BAL fluid compared with WT (Figure 5). Each of these sulfated glycan compositions exists as isomeric forms of the same mass (isobaric structures) that differ based on their sites of sialylation and sulfation. collision-induced dissociation (CID)-MS/MS was used to resolve the relative abundance of these isobaric species. Fragmentation of the *m/z* = 1386 precursor in WT and *CHST1*$^{-/-}$ BAL fluid produces identical MS^2/MS^3 spectra and support the presence of both 6-su-sLacNAc and 6-su-LacNAc arms on this core 2 glycan (Figure 6). Quantification of diagnostic fragments indicates that the relative abundance of the isobaric species is not different in WT and *CHST1*$^{-/-}$. Likewise, fragmentation of the *m/z* = 1835 precursor detects similar relative abundances of the isobaric forms of sulfated and sialylated glycans in the WT and *CHST1*$^{-/-}$ BAL fluid (Figure 7). For both of the major sulfated, sialylated O-glycan compositions detected in WT and *CHST1*$^{-/-}$ BAL fluid (*m/z* = 1386 and *m/z* = 1835), MS^3 fragmentation did not support the presence of 6′-su-sLacNAc motifs, the highest avidity Siglec-F ligand detected by in vitro glycan arrays (Yu et al. 2017). Rather, if the Gal residue of a LacNAc was sulfated, it was not also sialylated. And, if the Gal residue of a LacNAc was sialylated, sulfate was detected on the GlcNAc not the Gal, forming 6-su-sLacNAc.

Loss of CHST1 does not affect the abundance of siglec-F ligands in lung or BAL fluid

The abundance of Siglec-F ligands in the lung and trachea of WT and *CHST1*$^{-/-}$ mice was directly interrogated by probing blotted tissue lysates with Siglec-F–Fc. As previously reported (Kiwamoto et al. 2014, 2015), Siglec-F–Fc binding bands were detected at ≈500 kDa and ≈200 kDa in normal whole lung and trachea extracts. In lung and trachea of *CHST1*$^{-/-}$ mice, Siglec-F–Fc binding was comparable or increased compared with WT (Figure 8). In BAL fluid harvested from WT and *CHST1*$^{-/-}$ mice, Siglec-F–Fc binding was also not decreased in the *CHST1*$^{-/-}$ mice compared with WT and OVA challenge generated increased ligand expression at ≈500 kDa (Figure 8). The direct detection of Siglec-F ligands by Siglec-F–Fc blotting indicates that loss of *CHST1* does not decrease constitutive or OVA-induced synthesis of Siglec-F lung ligands.

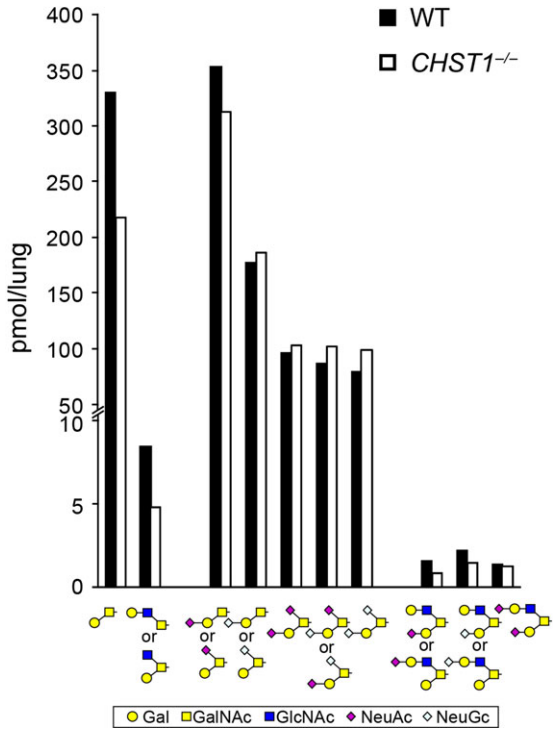

Fig. 2. O-glycans of wild-type and CHST1$^{-/-}$ lung tissue. Following release from lung proteins by reductive β-elimination, permethylated *O*-glycans were analyzed by NSI-MS (LTQ Orbitrap) and quantified relative to standard glycans of known amount. Compared with WT, the *CHST1*$^{-/-}$ mouse lung *O*-glycan profile is modestly enriched in more highly sialylated forms of the core 1 disaccharide. Graphical representation of monosaccharide residues are as shown in the boxed legend and are consistent with the Symbol Nomenclature for Glycans (SNFG). The presented profile is representative of two independent analyses of three pooled lungs for each genotype.

Loss of CHST1 does not affect the tissue distribution of siglec-F ligands in mouse lung

We next determined the localization of endogenous Siglec-F tissue ligands in the airway in WT and *CHST1*$^{-/-}$ mice using immunochemistry by probing with Siglec-F–Fc. As previously reported (Guo et al. 2011; Patnode, Cheng et al. 2013; Kiwamoto et al. 2014, 2015; Yu et al. 2017), expression of Siglec-F ligands was observed in airway epithelium in both OVA-challenged and phosphate-buffered saline (PBS)-challenged WT mice (Figure 9A). Furthermore, there were no obvious differences in patterns or intensity of Siglec-F ligand expression in airway epithelium in OVA-challenged and PBS-challenged WT and *CHST1*$^{-/-}$ mice. We also examined Siglec-F ligand expression in tracheal submucosal glands, and again saw no obvious differences in patterns or intensity of Siglec-F ligand expression before or after OVA challenge between WT mice and *CHST1*$^{-/-}$ mice (Figure 9B). These results indicate that both constitutive and allergen-induced production of lung ligands for Siglec-F by airway epithelium and in tracheal submucosal glands are independent of keratan sulfate galactose 6-*O*-sulfotransferase.

Loss of CHST1 alters cellular inflammatory responses in the airway

OVA sensitization and repeated intranasal challenge were performed on WT and *CHST1*$^{-/-}$ mice. Challenge of WT mice with OVA promoted an increase in total BAL cells that was attributable to increased neutrophil and eosinophil abundance (Figure 10, open bars). Challenge of *CHST1*$^{-/-}$ mice with OVA also promoted an increase in total BAL cells (Figure 10, black bars) and this increase was significantly greater than in OVA-challenged WT mice. Eosinophils and neutrophils also increased in the OVA-challenged *CHST1*$^{-/-}$ mice, but to the same degree as in the WT mice challenged with OVA. Instead, the greater increase in total BAL cells after OVA challenge in *CHST1*$^{-/-}$ mice compared with WT mice was due to a significant increase in macrophages and lymphocytes. These results indicate that absence of *CHST1* does not result in an alteration of allergen-driven accumulation of eosinophils (or neutrophils) into the mouse airway, but does result in enhanced accumulation of macrophages and lymphocytes.

Discussion

The binding of Siglec-F to glycan arrays demonstrated that sulfated sialyl LacNAc (su-sLacNAc) is a potent ligand for this anti-inflammatory receptor (Yu et al. 2017). More specifically, sulfation at the 6-position of the LacNAc Gal residue (6′-su-sLacNAc) generated a ligand for Siglec-F of the highest avidity. Therefore, the identification of a sulfotransferase capable of generating this high-avidity structure would produce a useful target for understanding the biosynthesis of anti-inflammatory glycans and for manipulating immunomodulatory glycan expression in lung disorders such as asthma (Kiwamoto et al. 2013). Keratan sulfate galactose 6-*O*-sulfotransferase (*CHST1*) is a reasonable candidate for production of the high-avidity 6′-su-sLacNAc ligands for Siglec-F. Therefore, we investigated whether this enzyme was necessary for the production of Siglec-F ligands in mice and whether a lack of 6′-su-sLacNAc might lead to enhanced allergic inflammatory responses in the lung.

Using *CHST1* homozygous deficient mice (*CHST1*$^{-/-}$) we investigated whether, as in mice lacking *St3gal3*$^{-/-}$ (Kiwamoto et al. 2014), loss of *CHST1* resulted in a more intense allergic eosinophilic airway inflammatory reaction and concomitant decrease in the production of high molecular weight Siglec-F ligands in their airways. Contrary to this hypothesis, *CHST1*$^{-/-}$ mice exhibit unaltered baseline and allergen-induced levels of Siglec-F ligands, consistent with a previous report that investigated parasite-induced lung inflammation using the same strain of *CHST1*$^{-/-}$ mice (Patnode, Cheng et al. 2013). A key implication of the findings reported here for OVA-induced inflammation and of the previously reported parasite-induced inflammation model is that endogenous lung ligands for Siglec-F may not contain 6′-su-sLe^{x} and 6′-su-LacNAc and that sulfation is not critical for Siglec-F binding. This observation is further supported by the fact that endogenous airway ligands for Siglec-F have been shown to be solvolysis-resistant on mucins, in particular Muc5b and Muc4, and that sialylated, multivalent LacNAc terminated glycans lacking sulfate are also potent ligands for Siglec-F based on glycan array screening (Kiwamoto et al. 2015). Furthermore, as demonstrated by Propster et al. (2016), amino acid residues within the lectin binding domain of Siglec-8, the human paralog of Siglec-F, necessary for 6′-sulfate recognition are conserved among primate siglecs but are not present in Siglec-F, consistent with our finding that sulfation is dispensable for Siglec-F ligand recognition in the airway.

While we detected a relatively minor decrease in one of the major sulfated core 2 *O*-glycans in *CHST1*$^{-/-}$ BAL fluid, MS^{n} fragmentation demonstrated that the sulfation position of this glycan and of the other sulfated glycans detected in BAL fluid were not 6′-sulfated Gal of a su-sLacNAc structure. Despite relatively unaltered

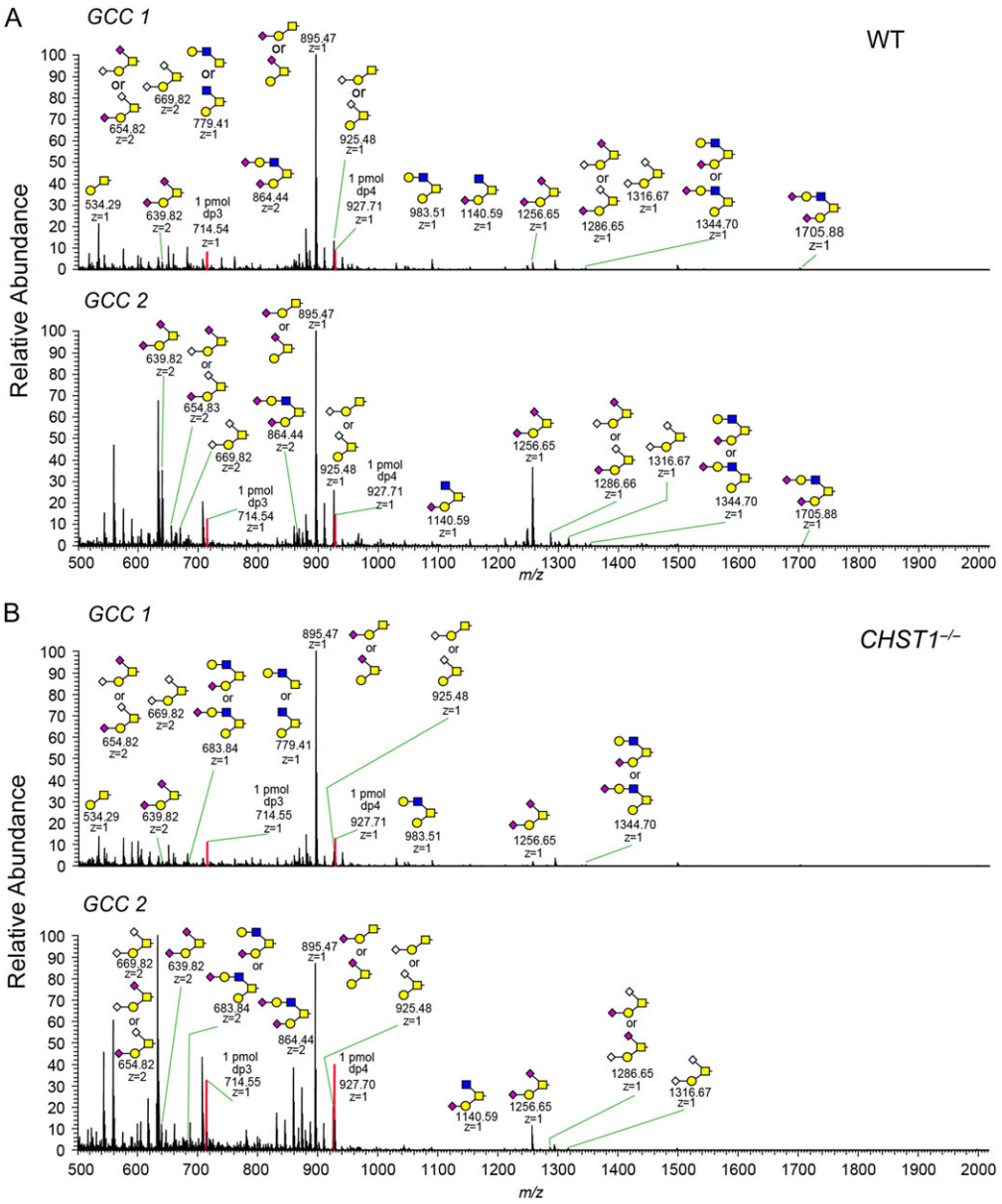

Fig. 3. Full MS profiles of *O*-glycans released from wild-type and *CHST1*$^{-/-}$ BAL fluid. Proteins were harvested from BAL fluid by acetone precipitation. Following release by reductive β-elimination, BAL fluid glycans were purified and fractionated on graphitized carbon columns, resulting in the generation of two fractions: GCC 1 containing primarily the neutral glycans that elute with 25% acetonitrile and GCC 2 containing the sialyalted and sulfated glycans that elute with 25% acetonitrile plus 0.05% trifluoroacetic acid (*GCC 1* and *GCC 2*). The fractionated *O*-glycans were permethylated and analyzed by NSI-MS (LTQ Orbitrap) in positive ion mode. Full MS profiles present the relative abundance of major O-glycans in WT (Panel **A**) and *CHST1*$^{-/-}$ (Panel **B**) BAL fluid. *O*-Glycans were detected as their sodiated species and primarily as singly charged ions, $m/z = (m + Na)^+$. The mass peaks corresponding to the quantification standards (permethylated maltotriose and maltotetraose; $m/z = 714.5$ and 927.7, respectively) are shaded red. The same amount of quantification standard was added to each sample.

mucin-type *O*-glycan sulfation in *CHST1*$^{-/-}$ mouse BAL fluid, sialylation of core 1 *O*-glycans was altered. The abundance of disialyl core 1 was reduced in *CHST1*$^{-/-}$ mouse BAL fluid, indicating that *CHST1* deficiency generates a collateral change in glycosylation that results in undersialylation of the secreted mucins found in BAL fluid. However, disialyl core 1 glycan is not a known ligand for Siglec-F.

Siglec-F lung ligands can be found on or in airway epithelium and submucosal glands, the latter found in the upper trachea (Guo et al. 2011; Patnode, Cheng et al. 2013; Kiwamoto et al. 2014, 2015; Yu et al. 2017). The lack of X-Gal labeling of airway epithelium is consistent with the lack of effect of deletion of *CHST1* on levels and localization of Siglec-F ligands in the lung reported here and elsewhere (Patnode, Cheng et al. 2013). Since we had previously reported that mouse airway epithelium stained with a polyclonal antiserum against keratan sulfate galactose 6-*O*-sulfotransferase (Guo et al. 2011), we can now only conclude that this staining was due to cross-reactivity of the antiserum with other proteins.

Eosinophilic and neutrophilic inflammation in the OVA model, like Siglec-F ligand expression, was also unaffected in *CHST1*$^{-/-}$ mice. Mouse neutrophils express Siglec-E rather than Siglec-F and

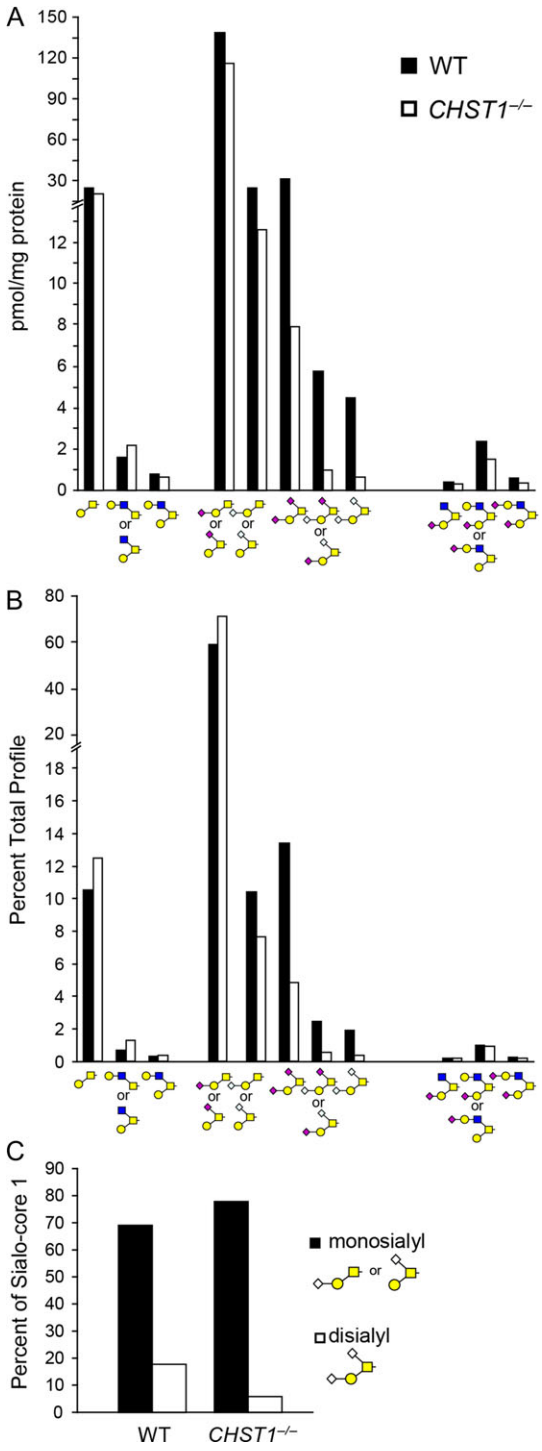

Fig. 4. *O*-glycans of wild-type and *CHST1*$^{-/-}$ BAL fluid. Released, permethylated *O*-glycans harvested from BAL fluid were quantified relative to standard glycans of known amount (Panel **A**). Compared with WT, the *CHST1*$^{-/-}$ mouse BAL fluid *O*-glycan profile is reduced in more highly sialylated forms of the core 1 disaccharide. This difference is also apparent when the abundance of each glycan is presented relative to the total glycan profile (% Total Profile, Panel **B**), indicating that a subset of glycans is impacted more than others by loss of *CHST1*. Quantification of the relative abundance of all monosialylated or disialylated glycans reveals that disialyl core 1 *O*-glycans are reduced by 67% in *CHST1*$^{-/-}$ BAL fluid compared with WT (Panel **C**). Unshaded diamonds in Panel C denote all forms of sialic acid (NeuAc and NeuGc). Quantification of released glycans is derived from a single BAL fluid sample harvested from each genotype.

Siglec-E recognizes 6-su-sLe^x but not 6′-su-sLe^x. The lack of impact of *CHST1* deficiency on neutrophil accumulation suggests that generation of Siglec-E ligands may be unaffected in this strain of mice as well. Such a conclusion is consistent with the finding that L-selectin-dependent trafficking of lymphocytes is normal in *CHST1*$^{-/-}$ mice, even though this enzyme is required to generate some 6-sulfated glycans (Patnode, Cheng et al. 2013).

An entirely unanticipated finding of this study was the enhanced accumulation of macrophages and lymphocytes after OVA challenge in *CHST1*$^{-/-}$ mice compared with WT mice. Whether distinct subsets of macrophages and lymphocytes were responsible for the increased accumulation remains to be determined. The underlying cause of macrophage and lymphocyte accumulation are not currently understood, but are unlikely to be due to Siglec-F because mouse lymphocytes have very little, if any, Siglec-F surface expression even during allergic inflammation responses (Zhang et al. 2007), and also because a deficiency of Siglec-F or Siglec-F ligands does not affect macrophage accumulation or survival in lung inflammation models (Zhang et al. 2007; Cho et al. 2010; Suzukawa et al. 2013; Kiwamoto et al. 2014). An intriguing hypothesis to be tested is whether the altered *O*-glycan sialylation that we detected in BAL fluid of *CHST1*$^{-/-}$ mice influences the anti-inflammatory activity of other Siglec receptors, especially those expressed on lymphocytes or macrophages. In this regard, the major Siglec of macrophages, Siglec-1/sialoadhesin, binds sialylated *O*-glycans on mucins.

In summary, *CHST1*$^{-/-}$ mice have similar amounts and patterns of distribution of Siglec-F ligands in their airways compared with WT mice. After OVA sensitization and challenge, *CHST1*$^{-/-}$ mice also have similar patterns of allergic granulocytic airway inflammation compared with WT mice, although the absence of *CHST1* results in exaggerated accumulation of airway macrophages and lymphocytes. Unlike the requirement for ST3Gal-III, keratan sulfate galactose 6-*O*-sulfotransferase neither contribute to the synthesis of glycan ligands for Siglec-F nor to the interaction between glycan ligands and Siglec-F in the airways. This finding is consistent with the concept that sialylated LacNAc structures presented as multivalent determinants, rather than 6′-su-sLe^x and 6′-su-LacNAc, act as the most biologically relevant, endogenous Siglec-F lung ligands. In addition, loss of *CHST1* impacts other glycosylation pathways such that secreted mucin proteins in BAL fluid exhibit altered *O*-glycan sialylation.

Materials and methods

Animals, ovalbumin sensitization and airway challenge

Mice employed in these experiments were 8–10 weeks old and included C57BL/6 mice (wild-type, WT) and *CHST1*$^{-/-}$ mice, the latter also on the C57BL/6 background and provided by the University of California, Davis via the Knock Out Mouse Project (www.komp.org). PCR-based genotyping was used to confirm homozygosity of the knockout mice. Mice were sensitized intraperitoneally with 50 µg of ovalbumin (OVA, Sigma-Aldrich, St. Louis, MO) in 1 mg alum on Days 1 and 8, then challenged intranasally with 20 µg OVA on Days 17, 19 and 21 to induce allergic airway inflammation. All mice were sacrificed 24 h after the final challenge. Control mice were injected and challenged with PBS. All procedures performed on mice were in accordance with the National Institute of Health guidelines for humane treatment and approved by the Johns Hopkins University Institutional Animal Use and Care Committee.

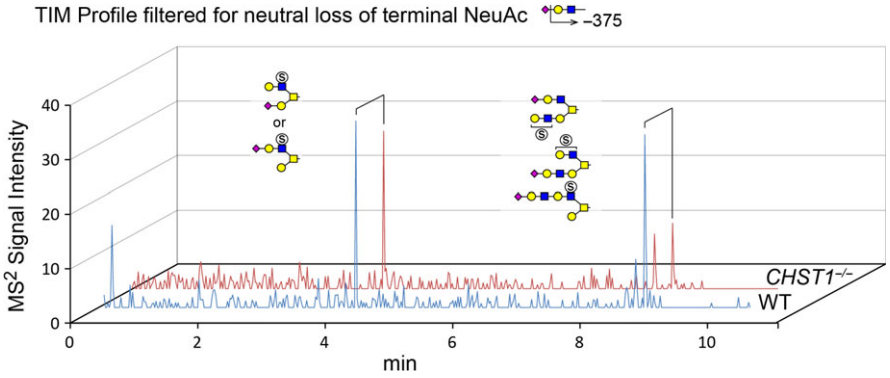

Fig. 5. Sulfo-glycans in BAL fluid. Sulfated glycans are extracted into an aqueous phase following permethylation. This enrichment enhances detection of sulfated glycans that are of low abundance compared with nonsulfated glycans in BAL fluid. Total ion mapping profiles generated in negative ion mode and filtered for MS^2 glycan fragment ions that underwent neutral loss of a sialic acid reveal the presence of two major sulfated, sialylated *O*-glycans. One of these, at $m/z = 1386$ is only slightly reduced in abundance in *CHST1*$^{-/-}$ BAL fluid compared with WT. The other, at $m/z = 1835$, is more substantially reduced.

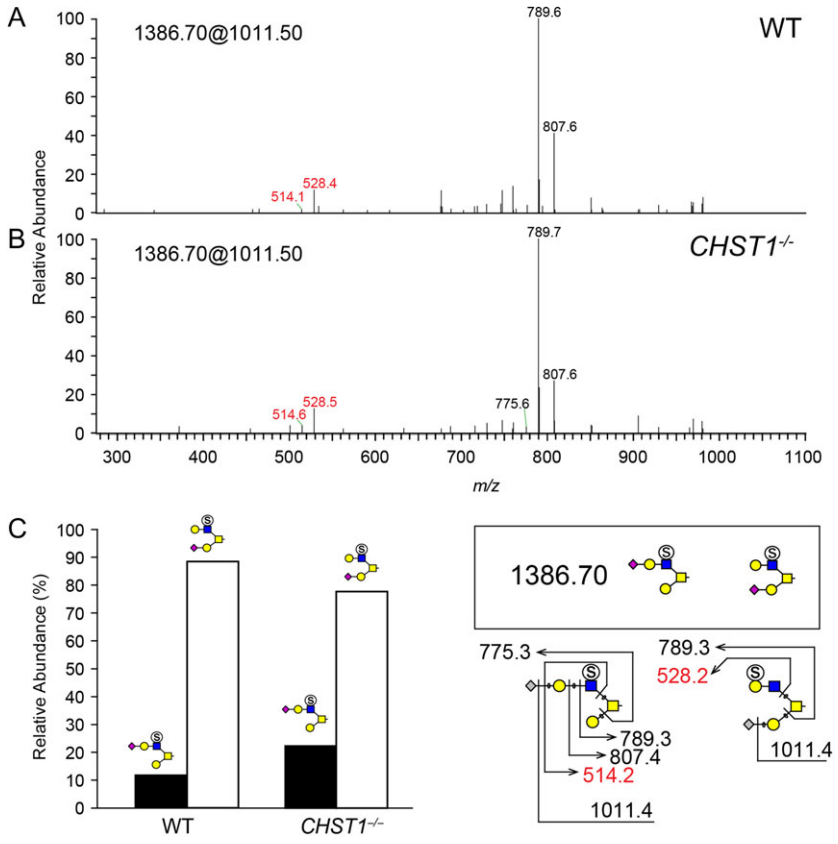

Fig. 6. Fragmentation of sulfated, sialylated glycan at $m/z = 1386$ detected in BAL fluid. The sulfated sialylated *O*-glycan at $m/z = 1386$ was accumulated in the ion trap of the LTQ Orbitrap mass spectrometer operating in negative ion mode and fragmented by CID. The MS^2 fragment ion at $m/z = 1011.5$, corresponding to loss of a terminal sialic acid residue, was selected for further fragmentation to assess isomeric complexity in the precursor peak. The MS^3 fragment profile was identical for WT (Panel **A**) and *CHST1*$^{-/-}$ (Panel **B**) glycans, indicating that the distribution of sulfated glycan isobars at this mass is unchanged in the absence of the enzyme. Fragmentation did not produce ions consistent with sulfation on the Gal residue of a sialylated LacNAc moiety (6′-su-sLacNAc). Quantification of the relative abundance of signature ions (shown in red in Panels A, B and in fragmentation diagram at lower right) for the dominant isobaric species indicates that *CHST1* is not responsible for production of the detected sulfation isomers (Panel **C**). The grayed diamond in the fragmentation diagram is meant to indicate that the sialic acid residue was lost in MS^2 prior to MS^3.

Nomenclature

Graphical representation of monosaccharide residues are as shown in the boxed legend for Figure 2 and are consistent with the Symbol Nomenclature for Glycans (SNFG), which has been broadly adopted by the glycomics community (Varki et al. 2015).

X-gal staining

Tissue distribution of *CHST1* was studied by immunohistochemistry with X-Gal staining because the deletion of the coding region of *CHST1* was accomplished by insertion of the LacZ and neomycin phosphotransferase genes (Patnode, Cheng et al. 2013; Patnode, Yu

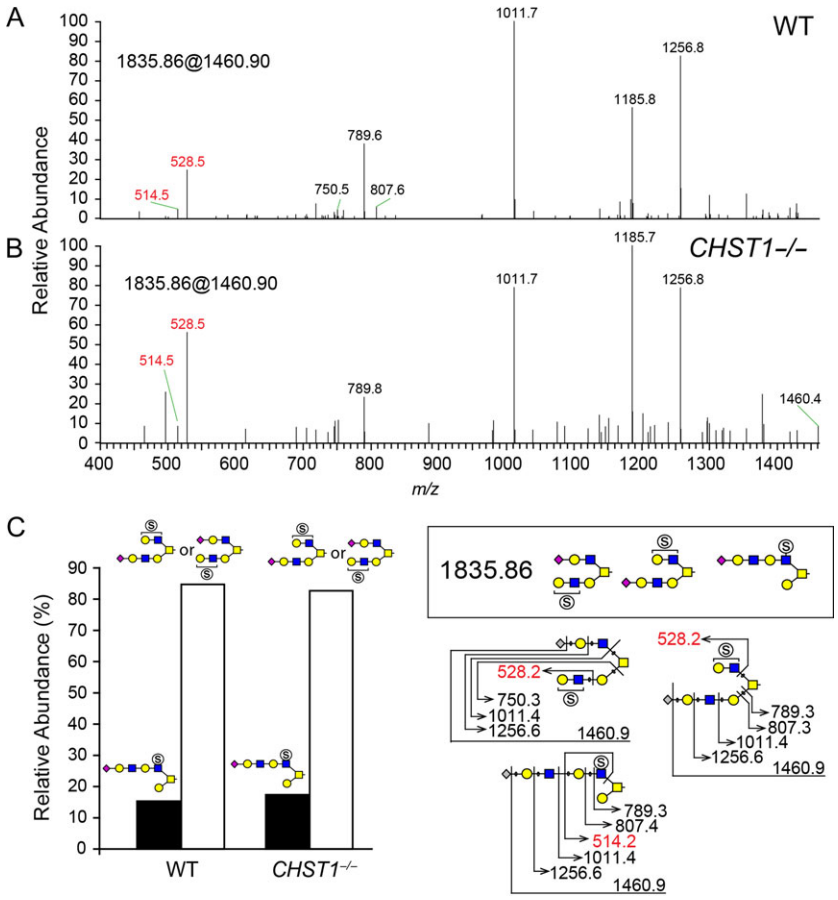

Fig. 7. Fragmentation of sulfated, sialylated glycan at *m/z* = 1835 detected in BAL fluid. The sulfated sialylated *O*-glycan at *m/z* = 1835 was accumulated in the ion trap of the LTQ Orbitrap instrument operating in negative ion mode and fragmented by CID. The MS^2 fragment ion at *m/z* = 1460.9, corresponding to loss of a terminal sialic acid residue, was selected for further fragmentation to assess isomeric complexity in the precursor peak. The MS^3 fragment profile was identical for WT (Panel **A**) and *CHST1*$^{-/-}$ (Panel **B**), indicating that the distribution of sulfated glycan isobars at this mass is unchanged in the absence of the enzyme. Fragmentation did not produce ions consistent with sulfation on the Gal residue of a sialylated LacNAc moiety (6′-su-sLacNAc). Quantification of the relative abundance of signature ions (shown in red in Panels A, B and in fragmentation diagram at lower right) for the dominant isobaric species indicates that *CHST1* is not responsible for production of the detected sulfation isomers (Panel **C**). The grayed diamond in the fragmentation diagram is meant to indicate that the sialic acid residue was lost in MS^2 prior to MS^3.

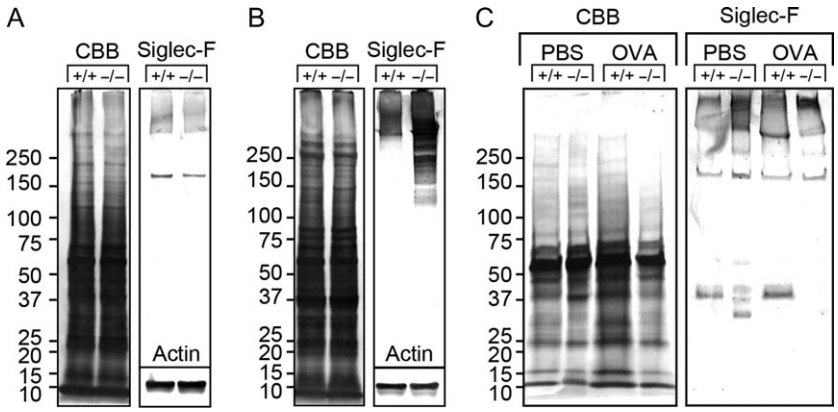

Fig. 8. Constitutive and OVA-induced expression of Siglec-F glycoprotein ligands detected by Siglec-F–Fc overlay. Equal amounts of lung (Panel **A**), trachea (Panel **B**) or BAL fluid (Panel **C**) protein harvested from WT or *CHST1*$^{-/-}$ mice were resolved by SDS-PAGE. The resulting gels were stained with Coomassie Blue (CBB) to assess protein equivalence or transferred to membranes and probed with Siglec-F–Fc (*Siglec-F*) to detect counter-receptor proteins that carry glycan ligands for Siglec-F. In all three biological materials, Siglec-F recognizes predominantly high molecular weight proteins previously identified as mucins, primarily Muc5b and Muc4. Loss of *CHST1* did not reduce Siglec-F binding in lung, trachea (Panels A, B), or BAL fluid, either at baseline or after OVA-induced airway inflammation (Panel C). The blots presented are representative of 2 (*CHST1*$^{-/-}$) and 3 WT independently-prepared tissue extracts.

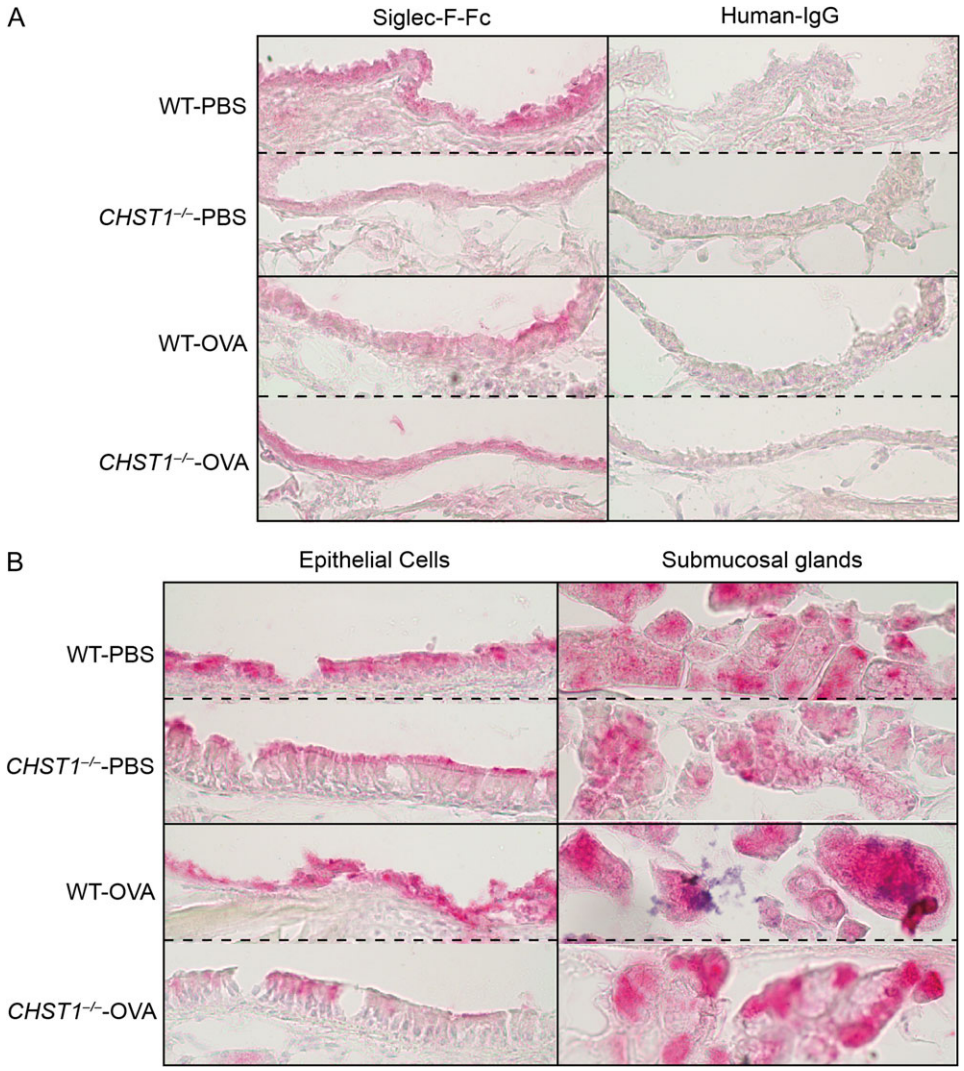

Fig. 9. Siglec-F ligand expression in the airways and tracheal submucosal glands of WT and *CHST*$^{-/-}$ mice. Representative photomicrographs of Siglec-F–Fc and human IgG control histochemistry of mouse airways demonstrating the specificity of the probe and the epithelial staining in the airway (Panel **A**), unlike the expression of *CHST1* (see Figure 1). Loss of *CHST1* did not eliminate Siglec-F binding in tracheal epithelium or in submucosal glands with or without OVA-induced airway inflammation (Panel **B**).

et al. 2013). Mouse lung and tracheal tissues were fixed, washed and stained overnight with X-Gal staining solutions (Millipore, Billerica, MA) according to the manufacturer's instructions. Stained tissues were incubated in 18% sucrose overnight then embedded in optimal cutting temperature compound (Sakura Finetek USA, Torrance, CA) and sectioned at 10 μm thickness.

Preparation of protein-enriched powder from lung and BAL fluid

For lung tissue, three whole lungs were combined prior to homogenization for each glycomic analysis. Two separate sets of three lungs were pooled from each genotype for replicate analysis. For BAL fluid, between 1.0 and 1.5 mL of fluid was harvested from each mouse and the entire volume from each mouse was used for glycomic analysis. Single samples of BAL fluid were obtained from each genotype for glycomic analysis. For both lung tissue and BAL fluid, protein-enriched powder was generated for glycan analysis as described previously (Aoki et al. 2007, 2008; Aoki and Tiemeyer 2010). Briefly, lungs were homogenized on ice in cold 50% methanol. The lysate was then adjusted to a ratio of chloroform:methanol:water::30:60:8 (v/v/v) and incubated at room temperature with agitation for at least 2 h. For BAL fluid, proteins were collected by acetone precipitation and the resulting pellet was resuspended in cold 50% methanol and subsequently extracted by adjusting the solvent mixture to chloroform:methanol:water::30:60:8 (v/v/v). Following centrifugation of lung or BAL fluid extracts at 2000 ×*g* for 15 min at 4°C, the resulting protein pellets were dried under a nitrogen stream and stored at −20°C until use.

Preparation of *O*-glycans

O-glycans were released from 5–7 mg of protein powder by reductive β-elimination as previously described (Aoki et al. 2008). Briefly, protein powder was incubated in 100 mM NaOH containing 1 M sodium borohydride for 18 h at 45°C. The reaction was then neutralized with 10% acetic acid on ice and desalted on a column of Dowex 50WX8 (H+ form). Released *O*-glycans were eluted with

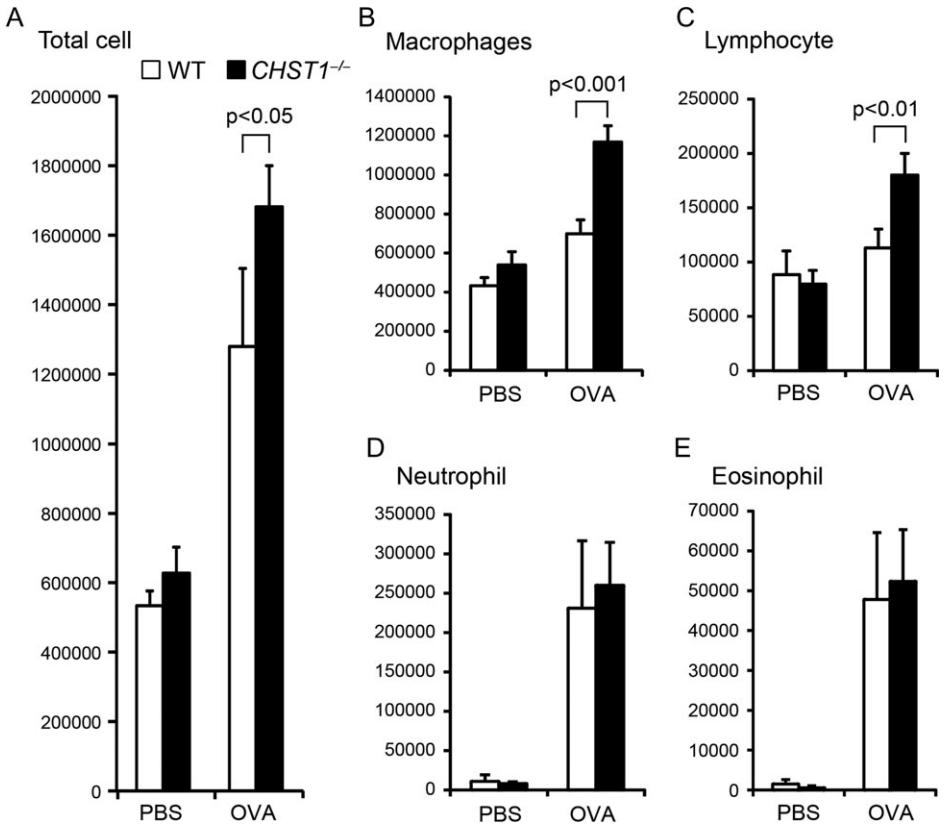

Fig. 10. BAL cell counts and differential in PBS and OVA-sensitized and challenged WT and *CHST1*$^{-/-}$ mice. BAL cells were obtained and analyzed 24 h after PBS or OVA final challenge. Total BAL cell number was increased in both WT and *CHST1*$^{-/-}$ mice that were OVA-sensitized and challenged compared with PBS control (Panel **A**). However, the increase in total cell number in the OVA-sensitized and challenged *CHST1*$^{-/-}$ mice was greater than in WT. This increased response in the *CHST1*$^{-/-}$ mice was attributable to greater numbers of macrophages and lymphocytes (Panels **B, C**). Increases in granulocytes were also detected in OVA-sensitized and challenged mice, but no difference was detected in the magnitude of the increase between WT and *CHST1*$^{-/-}$ mice (Panels **D, E**). n = 9–10, P-values are shown for changes of significance with $P < 0.05$.

5% acetic acid and lyophilized. Borate was removed by azeotrope with methanol; 10% acetic acid in methanol was added and the solution was dried under nitrogen stream, repeated three times. After borate removal, impurities were removed from the *O*-glycans by C18 column chromatography. Glycans eluted from the C18 column were lyophilized and dissolved in water. The dissolved *O*-glycans were applied to a pre-equilibrated graphitized carbon column. After washing with water, *O*-glycans were eluted in two steps, first with 25% acetonitrile (ACN; Fraction GCC 1) followed by 25% ACN containing 0.05% trifluoroacetic acid (Fraction GCC 2). The two fractions were lyophilized separately and stored at −80°C until permethylated prior to analysis.

Glycan permethylation

Released glycans were permethylated with methyliodide prior to MS analysis according to the method of Anumula and Taylor (1992). Known amounts of malto-series oligosaccharide standards (maltotriose and maltotetraose, dp3 and dp4, respectively) were permethylated with tri-deuterated CD_3I for use as external reference standards for quantification (Mehta et al. 2016).

Glycan mass spectrometry

Glycan samples were permethylated and analyzed by NSI-MS. For the detection and characterization of neutral and sialylated glycans laking sulfate, the permethylated glycans were reconstituted in 50% methanol containing 1 mM NaOH for infusion in positive ion mode and injected into a linear ion trap mass spectrometer with an orbital trap mass analyzer (LTQ Orbitrap; Thermo Fisher). For the detection and characterization of sulfated glycans, the permethylated glycans were reconstituted in methanol/2–propanol/1-propanol/13 mM aqueous ammonium acetate (16:3:3:2 by volume) for infusion in negative ion mode (Vukelic et al. 2005). The nanoelectrospray source was run at a syringe flow rate of 0.50 µL/min and capillary temperature set to 210°C (Aoki et al. 2007).

The LTQ Orbitrap instrument was tuned with a permethylated oligosaccharide standard in positive ion mode. For fragmentation by CID (in MS^2 and MS^n), normalized collision energy of 45% was applied. Most permethylated *O*-glycan components were identified as singly or doubly charged, sodiated species [M + Na] in positive mode. The intensities of dp oligosaccharide standards were used for quantification of individual glycans. Peaks for all charge states were deconvoluted by the charge state and summed for quantification. All spectra were manually interpreted and annotated. Permethylated glycans released from multiple biological preparations of protein powder were analyzed. The explicit identity of individual monosaccharide residues has been assigned based on the known biosynthetic pathways for mucin-type O-linked glycans in vertebrates. The MS-based glycomics data generated in these analyses and the associated annotations are presented in accordance with the MIRAGE

standards and the Athens Guidelines (Wells et al. 2013; York et al. 2014).

Siglec-F ligand expression

Detection of Siglec-F glycan ligands in lung-derived samples was determined by western blotting using a 4–15% polyacrylamide gel (Bio-Rad, Hercules, CA) as previously reported (Kiwamoto et al. 2014, 2015). Tissue distribution of Siglec-F glycan ligands was studied by immunohistochemistry with Siglec-F–Fc or isotype-matched humanized IgG1 monoclonal antibody and detected using an alkaline phosphatase imaging method as described previously (Guo et al. 2011; Kiwamoto et al. 2014, 2015).

Bronchoalveolar lavage cell enumeration

Mouse lungs were lavaged by repeated instillations of saline through a tracheal cannula. Cells in the lavage were enumerated exactly as done previously (Kiwamoto et al. 2014, 2015). Data are shown as means ± SEM. Statistical significance between groups was evaluated by analysis of variance and Tukey's multiple comparison test. *P*-values <0.05 were considered statistically significant.

Funding

This work was supported by the National Institutes of Health [AI72265 to B. S.B.; HL107151 to B.S.B., Z.Z., and M.T.; GM103490 to M.T.].

Conflict of interest statement

Dr. B.S.B. is a co-inventor on existing and pending Siglec-8-related patents and may be entitled to a share of future royalties received by Johns Hopkins University on the potential sales of such products. Siglec-8 is the human paralog of mouse Siglec-F, the subject of this manuscript. Dr. B.S.B. is also a co-founder of Allakos, Inc., which makes him subject to certain restrictions under University policy. The terms of this arrangement are being managed by the Johns Hopkins University and Northwestern University in accordance with their conflict of interest policies. Dr. B.S.B. has current or recent consulting or scientific advisory board arrangements with Sanofi-Aventis, Merck, GlaxoSmithKline, TEVA, and Allakos; and owns stock in Allakos and Glycomimetics, Inc. All other authors declare no competing financial interests.

Abbreviations

Su, Sulfate; LacNAc, N-acetyl-lactosamine (Gal-GlcNAc disaccharide); 6'-su-sLacNAc, 6'-sulfated sialyl N-acetyl-lactosamine; 6'-su-sLex, 6'-sulfated sialyl Lewis X; 6-su-sLacNAc, 6-sulfated sialyl N-acetyl-lactosamine; 6-su-LacNAc, 6-sulfated N-acetyl-lactosamine; BAL, bronchoalveolar lavage; CHST1, carbohydrate sulfotransferase 1, also known as keratan sulfate galactose 6-O-sulfotransferase; IL, interleukin; OVA, ovalbumin; PBS, phosphate-buffered saline; WT, wild type; NSI, nanospray ionization; MS/MS or MS2, tandem mass spectrometry; MSn, multi-dimensional mass spectrometry; CID, collision induced dissociation; ACN, acetonitrile GCC, graphitized carbon column.

References

Anumula KR, Taylor PB. 1992. A comprehensive procedure for preparation of partially methylated alditol acetates from glycoprotein carbohydrates. *Anal Biochem*. 203:101–108.

Aoki K, Perlman M, Lim J, Cantu R, Wells L, Tiemeyer M. 2007. Dynamic developmental elaboration of N-linked glycan complexity in the *Drosophila melanogaster* embryo. *J Biol Chem*. 282:9127–9142.

Aoki K, Porterfield M, Lee SS, Dong B, Nguyen K, McGlamry KH, Tiemeyer M. 2008. The diversity of O-linked glycans expressed during *Drosophila melanogaster* development reflects stage- and tissue-specific requirements for cell signaling. *J Biol Chem*. 283:30385–30400.

Aoki K, Tiemeyer M. 2010. The glycomics of glycan glucuronylation in *Drosophila melanogaster*. *Methods Enzymol*. 480:297–321.

Bochner BS. 2009. Siglec-8 on human eosinophils and mast cells, and Siglec-F on murine eosinophils, are functionally related inhibitory receptors. *Clin Exp Allergy*. 39:317–324.

Bochner BS, Alvarez RA, Mehta P, Bovin NV, Blixt O, White JR, Schnaar RL. 2005. Glycan array screening reveals a candidate ligand for Siglec-8. *J Biol Chem*. 280:4307–4312.

Cho JY, Song DJ, Pham A, Rosenthal P, Miller M, Dayan S, Doherty TA, Varki A, Broide DH. 2010. Chronic OVA allergen challenged Siglec-F deficient mice have increased mucus, remodeling, and epithelial Siglec-F ligands which are up-regulated by IL-4 and IL-13. *Respir Res*. 11:154.

Guo JP, Brummet ME, Myers AC, Na HJ, Rowland E, Schnaar RL, Zheng T, Zhu Z, Bochner BS. 2011. Characterization of expression of glycan ligands for Siglec-F in normal mouse lungs. *Am J Respir Cell Mol Biol*. 44:238–243.

Kiwamoto T, Brummet ME, Wu F, Motari MG, Smith DF, Schnaar RL, Zhu Z, Bochner BS. 2014. Mice deficient in the St3gal3 gene product α2,3 sialyltransferase (ST3Gal-III) exhibit enhanced allergic eosinophilic airway inflammation. *J Allergy Clin Immunol*. 133:240–247.

Kiwamoto T, Katoh T, Evans CM, Janssen WJ, Brummet ME, Hudson SA, Zhu Z, Tiemeyer M, Bochner BS. 2015. Endogenous airway mucins carry glycans that bind Siglec-F and induce eosinophil apoptosis. *J Allergy Clin Immunol*. 135:1329–1340, e1321-1329.

Kiwamoto T, Katoh T, Tiemeyer M, Bochner BS. 2013. The role of lung epithelial ligands for Siglec-8 and Siglec-F in eosinophilic inflammation. *Curr Opin Allergy Clin Immunol*. 13:106–111.

Mehta N, Porterfield M, Struwe WB, Heiss C, Azadi P, Rudd PM, Tiemeyer M, Aoki K. 2016. Mass Spectrometric Quantification of N-Linked Glycans by Reference to Exogenous Standards. *J Proteome Res*. 15: 2969–2980.

Na HJ, Hudson SA, Bochner BS. 2012. IL-33 enhances Siglec-8 mediated apoptosis of human eosinophils. *Cytokine*. 57:169–174.

Nutku E, Aizawa H, Hudson SA, Bochner BS. 2003. Ligation of Siglec-8: a selective mechanism for induction of human eosinophil apoptosis. *Blood*. 101:5014–5020.

Nutku E, Hudson SA, Bochner BS. 2005. Mechanism of Siglec-8-induced human eosinophil apoptosis: role of caspases and mitochondrial injury. *Biochem Biophys Res Commun*. 336:918–924.

Nutku-Bilir E, Hudson SA, Bochner BS. 2008. Interleukin-5 priming of human eosinophils alters Siglec-8 mediated apoptosis pathways. *Am J Respir Cell Mol Biol*. 38:121–124.

Patnode ML, Cheng CW, Chou CC, Singer MS, Elin MS, Uchimura K, Crocker PR, Khoo KH, Rosen SD. 2013. Galactose 6-O-sulfotransferases are not required for the generation of Siglec-F ligands in leukocytes or lung tissue. *J Biol Chem*. 288:26533–26545.

Patnode ML, Yu SY, Cheng CW, Ho MY, Tegesjo L, Sakuma K, Uchimura K, Khoo KH, Kannagi R, Rosen SD. 2013. KSGal6ST generates galactose-6-O-sulfate in high endothelial venules but does not contribute to L-selectin-dependent lymphocyte homing. *Glycobiology*. 23: 381–394.

Propster JM, Yang F, Rabbani S, Ernst B, Allain FH, Schubert M. 2016. Structural basis for sulfation-dependent self-glycan recognition by the human immune-inhibitory receptor Siglec-8. *Proc Natl Acad Sci USA*. 113:E4170–E4179.

Suzukawa M, Miller M, Rosenthal P, Cho JY, Doherty TA, Varki A, Broide D. 2013. Sialyltransferase ST3Gal-III regulates Siglec-F ligand formation and eosinophilic lung inflammation in mice. *J Immunol*. 190:5939–5948.

Tateno H, Crocker PR, Paulson JC. 2005. Mouse Siglec-F and human Siglec-8 are functionally convergent paralogs that are selectively expressed on eosinophils and recognize 6′-sulfo-sialyl Lewis X as a preferred glycan ligand. *Glycobiology*. 15:1125–1135.

Varki A, Cummings RD, Aebi M, Packer NH, Seeberger PH, Esko JD, Stanley P, Hart G, Darvill A, Kinoshita T et al. 2015. Symbol nomenclature for graphical representations of glycans. *Glycobiology*. 25: 1323–1324.

Vukelic Z, Zamfir AD, Bindila L, Froesch M, Peter-Katalinic J, Usuki S, Yu RK. 2005. Screening and sequencing of complex sialylated and sulfated glycosphingolipid mixtures by negative ion electrospray Fourier transform ion cyclotron resonance mass spectrometry. *J Am Soc Mass Spectrom*. 16:571–580.

Wells L, Hart GW, Athens Guidelines for the Publication of Glycomics D. 2013. Glycomics: building upon proteomics to advance glycosciences. *Mol Cell Proteomics*. 12:833–835.

York WS, Agravat S, Aoki-Kinoshita KF, McBride R, Campbell MP, Costello CE, Dell A, Feizi T, Haslam SM, Karlsson N et al. 2014. MIRAGE: the minimum information required for a glycomics experiment. *Glycobiology*. 24:402–406.

Yu H, Gonzalez-Gil A, Wei Y, Fernandes SM, Porell RN, Vajn K, Paulson JC, Nycholat CM, Schnaar RL. 2017. Siglec-8 and Siglec-9 binding specificities and endogenous airway ligand distributions and properties. *Glycobiology*. 27:657–668.

Zhang M, Angata T, Cho JY, Miller M, Broide DH, Varki A. 2007. Defining the in vivo function of Siglec-F, a CD33-related Siglec expressed on mouse eosinophils. *Blood*. 109:4280–4287.

Zimmermann N, McBride ML, Yamada Y, Hudson SA, Jones C, Cromie KD, Crocker PR, Rothenberg ME, Bochner BS. 2008. Siglec-F antibody administration to mice selectively reduces blood and tissue eosinophils. *Allergy*. 63:1156–1163.